Amphiphilic Poly(*p*-phenylene)-Driven Multiscale Assembly of Fullerenes to Nanowhiskers

Muhammad Hanafiah Nurmawati,[†] Parayil Kumaran Ajikumar,[†] Ravindranath Renu,[†] Chorng Haur Sow,[‡] and Suresh Valiyaveettil[†,‡,*]

[†]Department of Chemistry, and [‡]NUS—Nanoscience and Nanotechnology Initiative, National University of Singapore, 3 Science Drive 3, Singapore 117543

ARTICLE

ABSTRACT Molecular level alignment of components and optimum morphology of hybrid materials are of great interest in many applications. Morphology control has been extensively used as a direct tool in the evaluation of interactions and assemblies of components in thin films. It is believed that preparation method and composition are powerful tools to direct the morphology, particularly in self-assembled systems such as fullerene-based hybrid materials. The present report outlines a synergistic self-assembly of fullerenes (C_{60}) and functionalized poly (*p*-phenylene) (PPP) to develop nanofibers with high aspect ratios. Nanostructured PPP—C_{60} hybrids were prepared by direct casting of the dilute solution on solid substrates and on water under ambient conditions. The formation of whiskers with high aspect ratio and investigation of interesting photophysical properties are discussed. An amphiphilic PPP was used as a template for preparing nanohybrids of C_{60} at ambient temperature and conditions.

KEYWORDS: light-emitting polymers · amphiphilic poly(*p*-phenylene)s · fullerene · self-assembly · nanostructured whiskers

Multicomponent self-organization has been widely studied to create molecular level superstructures with various potential applications.[1–4] Recent interests in alternative energy sources warranted search for optimum donor—acceptor multicomponent hybrids such as π-conjugated macromolecules and fullerenes.[5] Micro- and nanostructuring of such systems are strongly affected by the chemical structure of the polymer, modified fullerene, and preparation methods.[6–11] Pioneering work by Goh *et al.* [12–15] consisted of using azide functional groups on various modified polymers to couple with fullerene and investigating the self-organization,[12] hydrophobic interactions between the components,[13] optical,[14] and mechanical[15] properties of the hybrid materials. In a recent review by Guldi *et al.*, covalent attachment of specific ionic and aromatic entities onto fullerenes have been shown to produce aggregate morphologies.[16] Also, controlling the size and morphology of fullerene-derived superstructures influences the properties and application of such materials.[17,18] For instance, interaction between donor polymer and acceptor fullerenes in bulk heterojunction photovoltaics led to significant improvement in the efficiency of the devices.[6] Curran *et al.*[7] have recently reported an increased solubility and exciton generation in poly(*m*-phenylenevinylene-*co*-2,5-dioctoxy-*p*-phenylenevinylene) (PmPV)/fullerene hybrid. The generation of excitons is believed to be responsible for many of the electronic properties found in most common and efficient polymer-based electronic devices.

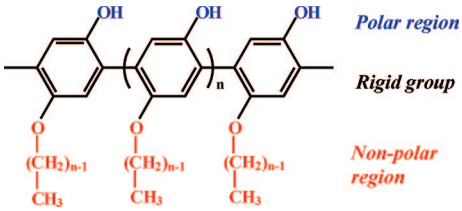

Figure 1. Chemical structure of amphiphilic poly(*p*-phenylene), C_nPPPOH.

The commonly adopted method for preparing bulk heterojunction layers involves spin coating the mixture from a homogeneous solution and annealing the film for optimum organization of two dissimilar components. Annealing helps the polymer chains to adopt energetically favorable architectures.[8] Recently, Manca *et al.* reported fabrication of a 2-D network of crystalline needles by spin coating a mixture of poly(3-hexylthiophene) (P3HT) and 6,6-phenyl-C_{61}-butyric acid methyl ester (PCBM) in chlorobenzene followed by annealing at 125 °C.[9] Although annealing processes showed reorganization of P3HT and PCBM to larger, well-organized microcrystalline assemblies, heating these materials at elevated temperatures may have unfavorable effects on the lifetime of the material/device. Thus, well-organized hybrid films prepared at ambient temperature are highly desirable for improved performance.[18]

Ⓦ This paper contains enhanced objects available on the Internet at http://pubs.acs.org/journals/ancac3.

*Address correspondence to chmsv@nus.edu.sg.

Received for review March 19, 2008 and accepted June 11, 2008.

Published online June 25, 2008.
10.1021/nn8001664 CCC: $40.75

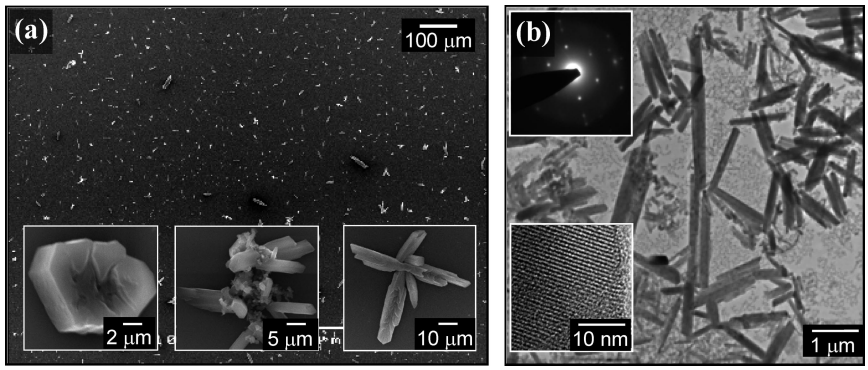

Figure 2. Micrographs of C_{60} crystallized from toluene solution (0.5 mg/mL): SEM (a) and TEM (b). The upper inset in panel b shows the electron diffraction pattern.

In the present study, self-organization of fullerenes with an amphiphilic poly(*p*-phenylene), C_nPPPOH (Figure 1) in ambient conditions was explored. Applications of the tailor-made C_nPPPOH toward the syntheses of organic and inorganic hybrid micro- and nanomaterials with interesting morphological and optical properties have been reported.[19–23] Weak interactions such as hydrogen bonds and alkyl chain crystallization were utilized for the cocrystallization of C_{60}−C_nPPPOH nanohybrid materials at ambient conditions. It would be interesting to note that the hydrogen-bond forming PPP polymer (C_nPPPOH) used in this study facilitated an extended conjugation in the PPP-based architectures,[20,23] which is advantageous for optimizing device performance.[24] It was anticipated that the rigid linear polymer, C_nPPPOH acted as a template for the crystallization of C_{60}. Strong interactions between the aromatic PPP backbone with C_{60} facilitated the formation of a well-dispersed polymer−fullerene nanohybrid.

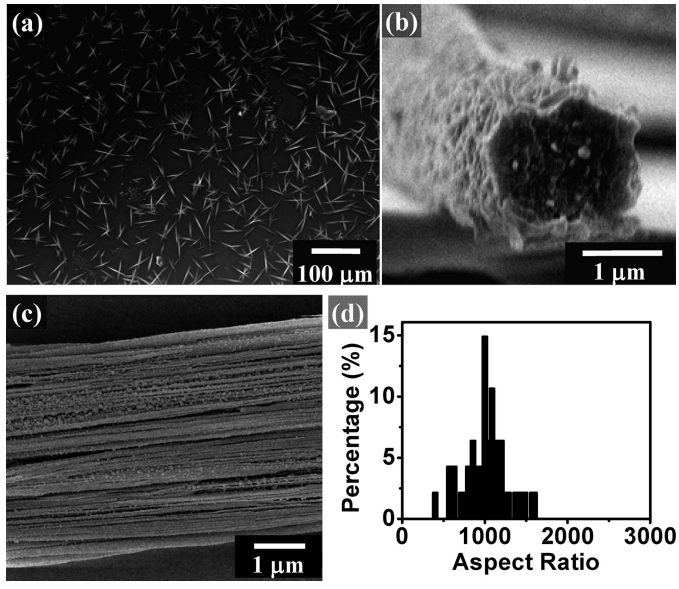

Figure 3. SEM micrographs of the whiskers cast from hybrid toluene solution (0.5 mg/mL) of 1:1 C_{60}:C_{12}PPPOH (a), cross section of a nanowhisker (b), and side view (c) of an individual nanowhisker showing multiple fibrils. The distribution of aspect ratio of nanofibers is given in panel d.

RESULTS AND DISCUSSION

Preparation and Characterization of Nanofibers. Developing high performance multicomponent polymer-C_{60} organic nanomaterials through supramolecular assemblies has remained a challenge owing to the poor dispersibility of C_{60} molecules in common solvents[25,26] and perturbation of its electronic properties[26] due to functionalization. The crystallization of unfunctionalized C_{60} molecules from solution shows that they have a strong tendency to aggregate into various sizes and morphologies.[10] Covalent and noncovalent functionalization of C_{60} has been extensively explored for facilitating the solubility in common solvents and influencing the assembly.[11,16] Ambient crystallization of C_{60} from a dilute solution (0.5 mg/mL in toluene) yielded multiple shapes and sizes (Figure 2).

Casting a solution of the mixture of C_{60} and C_{12}PPPOH (1:1, 0.5 mg/mL in toluene) onto a solid substrate induced unidirectional crystallization of nanohybrid material (Figure 3a) which led to the formation of nanofibers with high aspect ratios. Nanofibers that have an average diameter of 35 ± 5 nm and length of 30−50 μm aggregate to form whiskers. Magnified SEM micrographs show a cross section (Figure 3b) and side view (Figure 3c) of the whiskers with parallel-packed nanofibers. The observed high aspect ratio of 1050 (Figure 3d) is comparable to typical aspect ratios of carbon nanotubes (CNTs).

The higher level ordering of different components inside the fiber was investigated by high resolution TEM (HRTEM). HRTEM showed regular lattice fringes in the nanoneedles spanning along the growth axis (Figure 4a,b). Also apparent in Figure 4b is the highly regular lattice fringes. Such ordering is consistent with our previous observations that the dodecyloxy groups on the polymer C_{12}PPPOH direct the self-organization to form higher order structures such as micro-/nanostructured polymeric and nanohybrid thin films.[19,21] Planarization of the polymer backbone through potential O−H−O hydrogen bonds and optimum alkyl chain crystallization played an important role in the molecular level ordering of C_{12}PPPOH during the whisker formation. The first step of the multiscale assembly of the whisker formation involves a molecular level polymer−fullerene assembly driven by π−π stacking of the conjugated backbone of the polymer and the fullerene, resulting in the nanofibers. The calculated distance of 0.95 nm (calculated using HyperChemLite) between the adjacent polymer backbones (where π−π interactions with fullerenes are the strongest) is close to the diameter (0.72 nm) of the fullerenes. The next level nanofiber assembly led to the formation of large whisker-shaped superstructures.

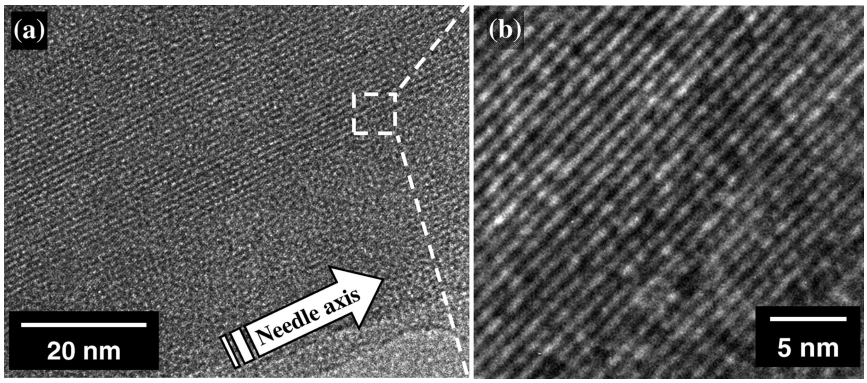

Figure 4. HRTEM image of the 1:1 C_{60}:C_{12}PPPOH nanohybrid prepared from 0.5 mg/mL toluene solution; along the needle axis (a) and lattice fringes (b).

The property of multicomponent hybrids is dependent on the blend ratio of its constituents. Recently, Yang *et al*. reported the increased phase segregation of PCBM-rich areas in annealed samples with PCBM content from 20% to 80% with respect to the polymer content.[17] We have prepared C_{12}PPPOH-C_{60} nanohybrid whiskers with increased amounts of C_{60} as well as different ratios of C_{12}PPPOH and C_{60}. A homogeneous loading of 100−200% unfunctionalized C_{60} (5−10 mg/mL) with respect to polymer content led to the formation of nanofibers with high aspect ratios (Figure 5a,b). The higher loading of C_{60} in the polymer matrix is facilitated by the improved solubility of unfunctionalized C_{60} in C_{12}PPPOH solution. Similarly, increasing the concentration of C_{12}PPPOH and C_{60} (1.0 mg/mL) with constant blend ratio yielded more whiskers without significant alterations in the morphology or the aspect ratio (Figure 5c).

Morphology Control of Nanofibers. Adjusting the kinetics of solvent evaporation during the direct casting allowed us to fine-tune the length and width of the nanorods and whiskers (Figure 6). Retarding the growth rate of the whiskers by evaporating the nanohybrid solution within a confined volume resulted in a 5-fold increase in the aspect ratio. On the other hand, increasing the growth rate by evaporation of the solvent under centrifugal force of spin coating led to a 5-fold decrease in the aspect ratios.

Our previous studies reported that a facile microstructuring of C_{12}PPPOH thin films into well-ordered honeycomb arrays is possible with a volatile solvent such as chloroform.[21] Substantial morphology control of the nanohybrid whiskers could additionally be achieved *via* solvent mixtures. For example, when a 50:50 volume ratio of toluene and chloroform was used, self-organized whiskers with a high aspect ratio were integrated into the honeycomb structures with a high degree of directionality (Figure 7). No significant changes in morphology were observed due to the C_{60} crystallization. A control experiment carried out using the same solvent system but in the absence of polymer in the casting solution yielded rod-like structures of variable size, comparable to those cast from toluene solution (Figure 2).

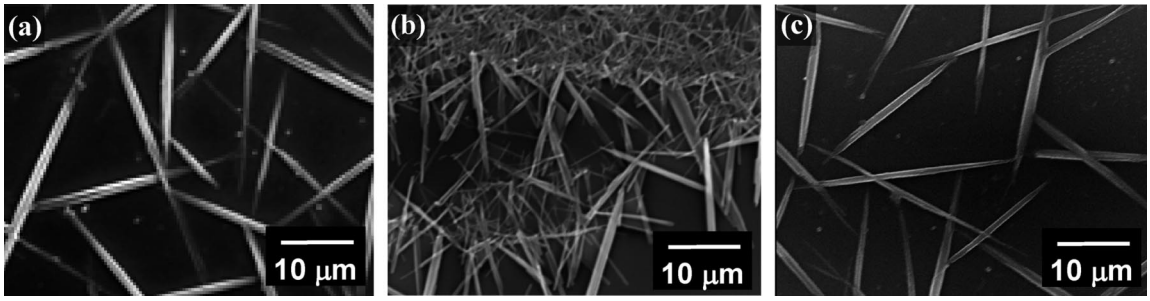

Figure 5. SEM micrographs of nanohybrid whiskers prepared using 0.5 mg/mL toluene solution of 1:2 blend ratio of C_{60}:C_{12}PPPOH (a), 0.5 mg/mL of 1:10 blend ratio of C_{60}:C_{12}PPPOH (b) and 1.0 mg/mL of 1:1 blend ratio of C_{60}:C_{12}PPPOH (c).

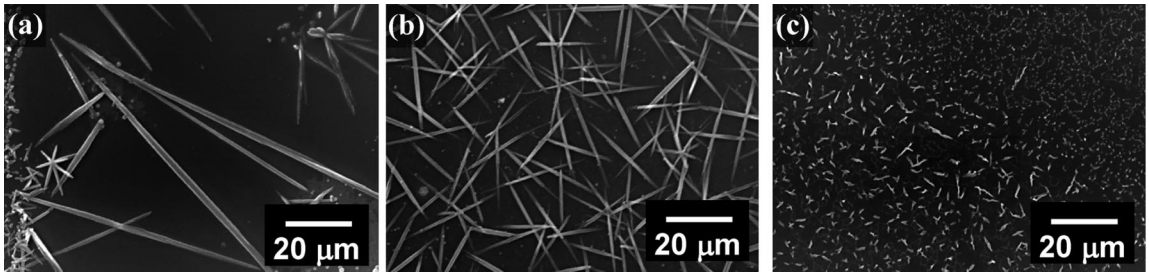

Figure 6. SEM micrographs of 1:1 C_{60}:C_{12}PPPOH nanohybrid whiskers prepared from 0.5 mg/mL toluene solution; formed inside an enclosed desiccator (a), in ambient (b), and with spin coating of a nanohybrid solution at 1000 rpm (c).

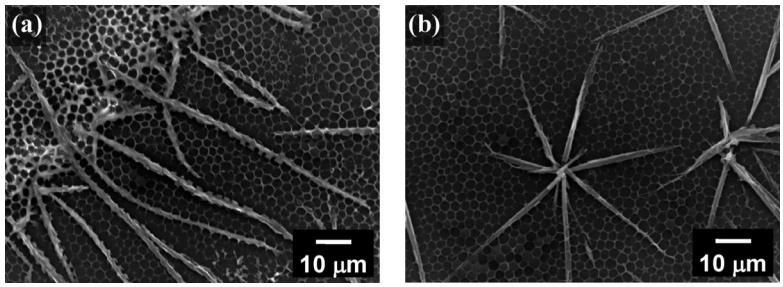

Figure 7. SEM micrographs of 1:1 C_{60}:C_{12}PPPOH nanohybrid whiskers using 0.5 mg/mL of 50% toluene/$CHCl_3$ solvent at the periphery (a) and center (b) of nanohybrid film.

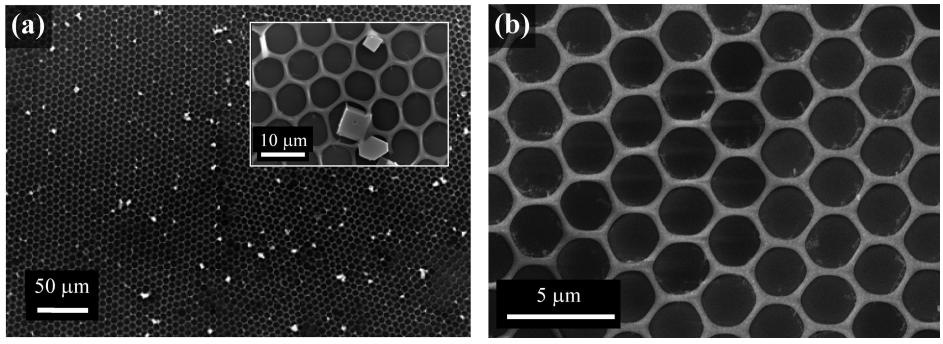

Figure 8. SEM micrographs of 0.5 mg/mL 1:1 C_{60}:C_{12}PPPOH nanohybrid casted from $CHCl_3$ solution (a) and 85% v/v CS_2/$CHCl_3$ solution (b).

In contrast, the mixture of C_{12}PPPOH−C_{60} cast from chloroform solution resulted in highly ordered honeycomb arrays of polymer film (no distinct directional ordering due to rapid evaporation) with cuboctahedral fullerene structures (Figure 8a). This is consistent with the previous studies which demonstrated that C_{60} crystallizes from chloroform solution into symmetrical stacks of cuboctahedral structures.[10] Using an optimum solvent mixture of 85% v/v CS_2/$CHCl_3$ led to controlled crystallization of C_{60} to develop a large area of periodic and intricately patterned nanohybrid thin films with fullerenes integrated into the honeycomb matrix (Figure 8b). Thus by choosing an appropriate polymer and solvent mixture, the size and shape of the nanohybrid materials could be fine-tuned.

Directional Growth of Nanofibers. To understand the crystallization process and growth mechanism, real time video microscopy was performed. (See Video 1, Video 2, Video 3, Video 4, and Video 5 as web enhanced objects on the online version of this article.) The growth of whiskers was observed with good reproducibility in multiple experiments. Due to the fast evaporation of solvent at the solvent front, crystal growth started at the edge and moved toward the center of the drop (Figure 9a). Growth with inward orientation (Figure 9b) continued until saturation was reached, where multitudes of whiskers formed in random directions (Figure 9c). The number of whiskers developed in the oriented region was generally lower as compared to other regions. There is approximately 20% increase in the abundance of whiskers per unit area in randomly oriented region. In addition to the free growth, directed growth of whiskers was studied using TEM grids and tungsten wire to demonstrate controlled crystallization.

To demonstrate the influence of alkoxy groups toward the formation of nanowhiskers, polyhydroxylated PPP with hexyloxy group on the backbone (C_6PPPOH) was synthesized. Whiskers with high aspect ratios were clustered and showed an uncontrolled crystallization (Figure 10a). Polymer with shorter alkyl chains, for example, C_6PPPOH, solidifies faster into less-organized structures owing to the low solubility in organic solvents. Moreover, the supramolecular organization of PPP with shorter and longer chains in solution can be expected to be different in micro/nanostructured thin films of C_nPPPOH.[20,21] The dodecyloxy chain of C_{12}PPPOH is optimum for efficient packing in the short period of solvent evaporation (typically in 60−120 s) which in turn induced synergistic self-organization with fullerenes. These observations are consistent with the previous report from Shinkai *et al.*, where a decrease in the chain length of solvophilic polystyrene in a poly(styrene-*b*-4-vinylpyridine) copolymer caused a reduction in the surface area for accommodating fullerene superstructures.[27]

Earlier studies on the structure−property relationship of a series of C_nPPPOH polymer revealed that the polymer bearing dodecyloxy group (C_{12}PPPOH), showed better film forming and opto-

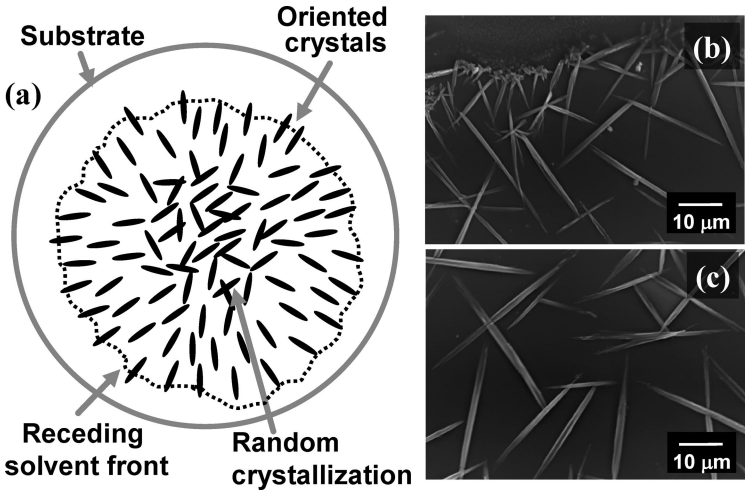

Figure 9. Schematic (a) and SEM micrographs of (b) inward and (c) random orientation of 1:1 C_{60}:C_{12}PPPOH nanohybrids prepared from 0.5 mg/mL toluene solution.

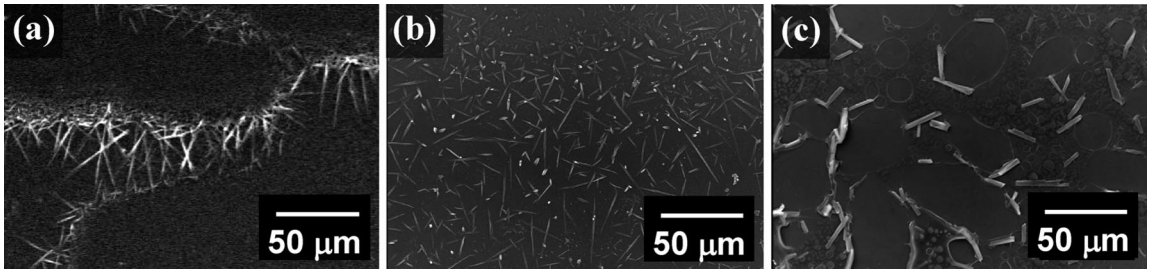

Figure 10. SEM images of nanohybrid whiskers prepared using 0.5 mg/mL of 1:1 blend ratio of C_{60} with C_6PPPOH (a), C_{12}PPPOBn (b), and PMMA (c).

electronic properties.[19,20] Planarization of the backbone through hydrogen bonding and alkyl chain crystallization played a significant role in the molecular level ordering inside the film. In a control experiment, polymer C_{12}PPPOBn, in which hydroxyl groups were protected by a benzyl group, yielded very small needle structures of 5−10 μm in length (Figure 10b). Nonconjugated poly(methylmethacrylate) (PMMA) resulted in C_{60} aggregates of irregular shapes and sizes, similar to crystals prepared from C_{60} solution (Figure 10c). The aforementioned studies confirmed that the intricate balance in molecular orientation, driven by subtle noncovalent interactions, played an important role in the self-organization process.

Photophysical Properties of Nanofibers. Polymer film dropcast from a 0.5 mg/mL C_{12}PPPOH toluene solution provided featureless blue emitting images under UV exposure using a mercury lamp (excitation at 365 ± 12 nm) of a confocal microscope (Figure 11a). In a similar approach, pure C_{60} crystals did not show emission under the same condition. A homogeneous mixture of C_{12}PPPOH and C_{60} in a 1:1 ratio showed significant reduction in the emission (Figure 11b). After excitation, the polymer showed a broad emission at a wavelength range of 360−530 nm, which is absorbed by C_{60} molecules within the whiskers at a wavelength up to 400 nm. Such efficient energy transfer was possible owing to the highly ordered and close molecular level organization of all components in the nanohybrid (Figure 4). Strong π−π interactions between C_{60} and C_{12}PPPOH aromatic backbone, coupled with the excellent self-assembling properties of C_{12}PPPOH also enhances the mixing of individual components at the interface. The confocal images taken under UV excitation of nanohybrid whiskers of C_{12}PPPOH-C_{60} are shown in Figure 12a,b. Accordingly, quenched emission of the whiskers shows the homogeneity of the nanohybrid crystals, and brighter regions surrounding the whiskers seen in the same figure indicate the presence of free polymer wrapping around the self-assembled nanofibers (Figure 12a,b). The brightfield images (Figure 12c,d) with no UV-excitation showed the morphology of the crystals. It is also clear that the nucleation and growth of the whiskers originated from a supersaturated region with high concentration of polymers and C_{60}.

Proposed Mechanism of Nanofiber Formation. There are two stages in the growth of whiskers (Figure 9). The initial stage involved the cocrystallization of C_{12}PPPOH and C_{60} along the solvent front of the solution, as evaporation take place continuously. The whiskers formed during this stage are therefore directed along the receding solvent front (Figures 9b, 12b, and 12d). Upon reaching saturation, instantaneous nucleation and growth of whiskers were observed. Due to the nature of solvent evaporation and rapid growth of crystals, cocrystallization led to randomly oriented whiskers without change in morphology or bundling of the nanofibers.

The observed characteristics of long-range ordering of the polyhydroxylated PPPs with C_{60} stem from the unique structure and self-assembly of C_{12}PPPOH. This polymer and a few more derivatives are being investigated owing to their ability to organize nanomaterials without loosing the inherent properties of the polymer[19,21] as well as hybrids.[22] Experimental data suggest that synergistic interactions led to translational ordering inside the polymer lattice with multiple periodicities. The first level of organization involves the molecular level polymer−fullerene complex formation driven by π−π stacking of the conjugated polymer backbone and C_{60}, which then led to the formation of nanofibers with 35 ± 5 nm widths and 30−40 μm length. The next level of organization involved the assembly of nanofibers to form large whiskers. High periodicity found by electron diffraction is related to the stacking of C_{60} along the PPP backbone aligned parallel to the whisker axis.

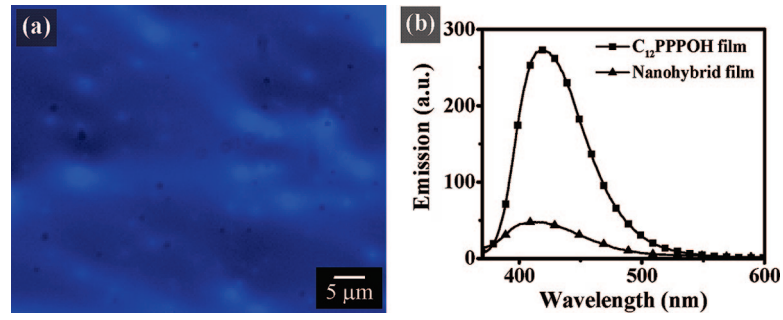

Figure 11. Confocal image of C_{12}PPPOH dropcast film prepared from 0.5 mg/mL toluene solution under UV excitation (a) and emission (b) spectra of polymer and nanohybrid films.

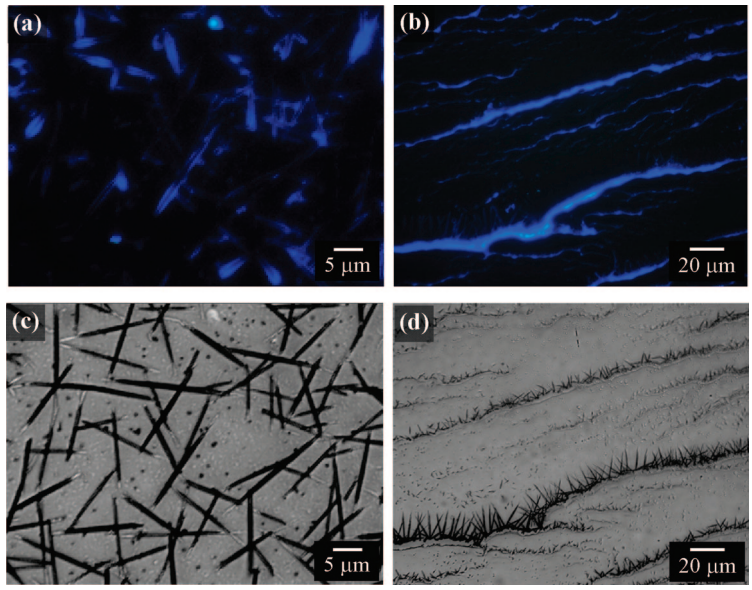

Figure 12. Confocal micrographs of 1:1 C_{60}:C_{12}PPPOH nanohybrid whiskers prepared from 0.5 mg/mL toluene solution (a) and the formation of the whiskers at the receding solvent front (b) under the UV exposure. The corresponding micrographs of the nanowhiskers with no UV exposure (c) and the solvent front contours (d) show the morphology. The blue emission is due to the presence of C_{12}PPPOH polymer.

A plausible supramolecular organization is proposed on the basis of the understanding of strong interchain hydrogen bonding and $\pi-\pi$ interactions between the planarized polymer backbones with fullerenes (Figure 13).[20,23] A significant interplay of specific hydrophobic, hydrophilic, and other weak interactions acting within the system[3,11–13] may be the driving force in forming highly ordered crystallites of C_{60} and their nanohybrids during the short duration of solvent evaporation. The absence of such features in other polymers led to significant changes in the morphology and structure of the whiskers (Figure 10). It is conceivable that the orientation of bundled nanofibers (whiskers) is influenced by the kinetics of solvent evaporation.

CONCLUSIONS

Casting a solution of C_{60} and C_{12}PPPOH onto substrates induced unidirectional cocrystallization of C_{12}PPPOH–C_{60} nanohybrids which led to the formation of nanofibers with high aspect ratios. The morphological and optical properties from this study showed an alternative method to tailor the fullerene–polymer interactions without using covalently functionalized C_{60} or high temperature post-treatment. In the light of the importance of achieving strong control over nanoscale morphology in the electronic applications of interesting organic and hybrid materials, this report signifies an essential prerequisite in thoroughly understanding the fullerene–polymer interactions and their multiscale assembly in ambient conditions. It is anticipated that a careful interface engineering of various components inside a nanohybrid system

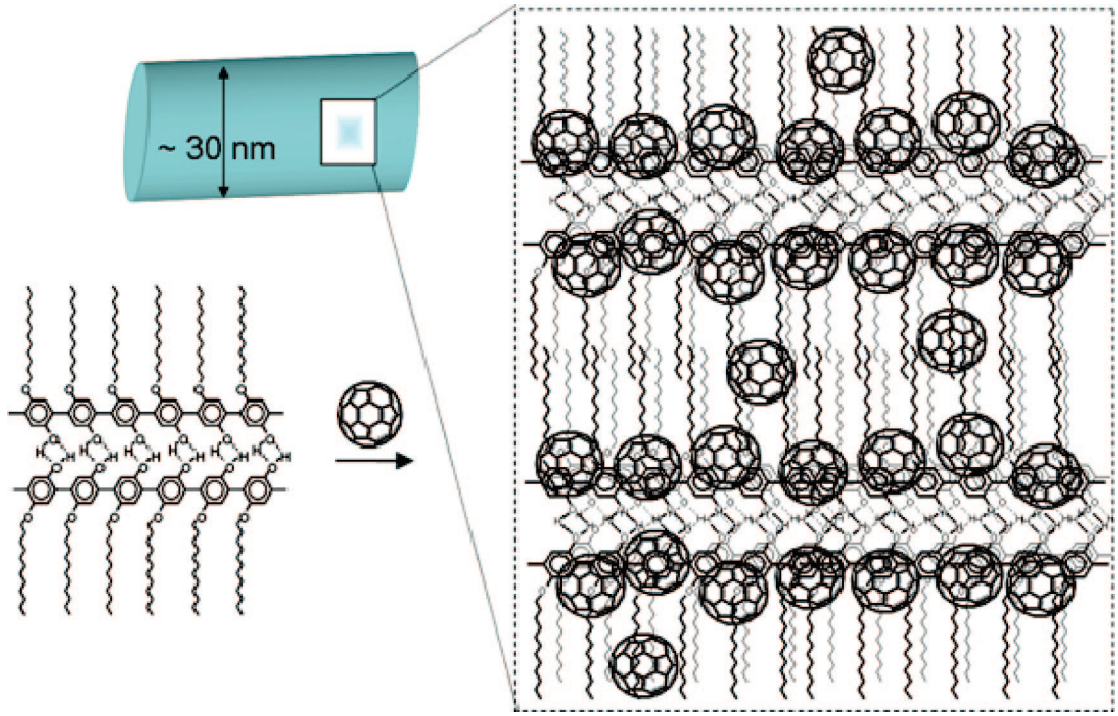

Figure 13. Proposed illustration of a long-range order inside the nanowhiskers under dynamic equilibrium, directed by hydrophobic (alkyl chain–fullerene), $\pi-\pi$ interaction and hydrogen bonding inside the lattice.

through interplay of weak interactions will allow us to generate or optimize interesting properties of materials. Further studies of C_{12}PPPOH directed self-organization of multicomponent systems consisting of C_{60} or semiconducting quantum dots are in progress.

EXPERIMENTAL METHODS

Amphiphilic poly(*p*-phenylenes) C_6PPPOH, C_{12}PPPOH, and C_{12}PPPOBn were synthesized using the Pd(0) catalyzed Suzuki polycondensation as reported earlier and well characterized.[23] Stock solutions of the different polymers (1.0 mg/mL) were prepared in toluene. A predetermined amount of fullerene (SES Research) was weighed and mixed with the polymer solution. The solutions were then used for direct spreading onto solid substrates and water surface. The nanostructured solid films were characterized using scanning electron and laser scanning confocal microscope.

SEM images were taken with a JEOL JSM 6700 scanning electron microscope (SEM). The samples were carefully mounted on copper stubs with a double-sided conducting carbon tape and sputter-coated with 2 nm platinum, before examination. TEM images were taken using JEOL JEM 2010F at an accelerating voltage of 200 keV and HRTEM images were obtained using JEOL JEM 3010 at an accelerating voltage of 300 keV. The film was cast on water and carefully transferred onto a 400 mesh carbon-coated copper grid for imaging. For the fluorescence imaging, a Carl Zeiss LSM 510 laser scanning microscope with a source operating at an excitation wavelength of 365 $\pm$ 12 nm was used. The solution and solid state UV absorbance measurements were done using Shimadzu 3101 PC and the corresponding photoluminescence studies were carried out using Shimadzu RF-5301PC fluorescence spectrophotometer. The real-time imaging process of the self-organization was captured using a Nikon measuring microscope MM-40 attached with Nikon Coolpix E995 camera.

Acknowledgment. This work was supported by National University of Singapore, Agency for Science, Technology and Research (ASTAR) and Singapore-MIT Alliance, Singapore. The authors acknowledge the technical support from the Departments of Chemistry and Physics at the National University of Singapore. The authors also thank Dr. Gudipati, C. S. for kind help in proof reading the manuscript.

REFERENCES AND NOTES

1. Whitesides, G. M.; Grzybowski, B. Self-Assembly at All Scales. *Science* **2002**, *295*, 2418–2421.
2. Zheng, W.; Jacobs, H. O. Self-Assembly Process to Integrate and Connect Semiconductor Dies on Surfaces with Single-Angular Orientation and Contact-Pad Registration. *Adv. Mater.* **2006**, *18*, 1387–1392.
3. Malenfant, P. R. L.; Wan, J.; Taylor, S. T.; Manoharan, M. Self-Assembly of an Organic−Inorganic Block Copolymer for Nano-Ordered Ceramics. *Nat. Nanotechnol.* **2007**, *2*, 43–46.
4. Zuruzi, A. S.; Ward, M. S.; MacDonald, N. C. Fabrication and Characterization of Patterned Micrometre Scale Interpenetrating Au−TiO_2 Network Nanocomposites. *Nanotechnology* **2005**, *16*, 1029–1034.
5. McGehee, M. D.; Topinka, M. A. Solar cells: Pictures from the Blended Zone. *Nat. Mater.* **2006**, *5*, 675–676.
6. Sivula, K.; Ball, Z. T.; Watanabe, N.; Fréchet, J. M. J. Amphiphilic Diblock Copolymer Compatibilizers and Their Effect on the Morphology and Performance of Polythiophene:Fullerene Solar Cells. *Adv. Mater.* **2006**, *18*, 206–210.
7. Wondmagegn, W. T.; Curran, S. A. A Study of C_{60}-Poly(*m*-phenylenevinylene-*co*-2,5-dioctoxy-*p*-phenylenevinylene) Nanocomposite. *Thin Solid Films* **2006**, *515*, 2393–2397.
8. Hoppe, H.; Sariciftci, N. S. Morphology of Polymer/Fullerene Bulk Heterojunction Solar Cells. *J. Mater. Chem.* **2006**, *16*, 45–61.
9. Swinnen, A.; Haeldermans, I.; Ven, M. V.; D'Haen, J.; Vanhoyland, G.; Aresu, S.; D'Olieslaeger, M.; Manca, J. Tuning the Dimensions of C_{60}-Based Needlelike Crystals in Blended Thin Films. *Adv. Funct. Mater.* **2006**, *16*, 760–765.
10. Saha, A.; Mukherjee, A. K. Cuboctahedral Symmetry in the Aggregation of [60]Fullerene in Polar Organic Media. *J. Chem. Phys.* **2005**, *122*, 184504.
11. Georgakilas, V.; Pellarini, F.; Prato, M.; Guldi, D. M.; Melle-Franco, M.; Zerbetto, F. Supramolecular Chemistry and Self-Assembly Special Feature: Supramolecular Self-Assembled Fullerene Nanostructures. *Proc. Natl. Acad. Sci. U.S.A.* **2002**, *99*, 5075–5080.
12. Huo, H.; Ngai, T.; Goh, S. H. Self-Organization of Double-C_{60} End-Capped Poly(ethylene oxide) in Chloronaphthalene and Benzene Solvent Mixtures. *Langmuir* **2007**, *23*, 12067–12070.
13. Song, T.; Goh, S. H.; Lee, S. Y. Interpolymer Complexes Through Hydrophobic Interactions: C_{60}-End-Capped Linear or Four-Arm Poly(ethylene oxide)/Poly(acrylic acid) Complexes. *Macromolecules* **2002**, *35*, 4133–4137.
14. Elim, H. I.; Ouyang, J. Y.; Goh, S. H.; Ji, W. Optical-Limiting-Based Materials of Mono-Functional, Multi-Functional and Supramolecular C_{60}-Containing Polymers. *Thin Solid Films* **2005**, *477*, 63–72.
15. Wang, M.; Pramoda, K. P.; Goh, S. H. Reinforcing and Toughening of Poly(vinyl chloride) with Double-C_{60}-End-Capped Poly(*n*-butyl methacrylate). *Macromolecules* **2006**, *39*, 4932–4934.
16. Guldi, D. M.; Zerbetto, F.; Georgakilas, V.; Prato, M. Ordering Fullerene Materials at Nanometer Dimensions. *Acc. Chem. Res.* **2005**, *38*, 38–43.
17. Yang, X.; van Duren, J. K. J.; Janssen, R. A. J.; Michels, M. A. J.; Loos, J. Morphology and Thermal Stability of the Active Layer in Poly(*p*-phenylenevinylene)/Methanofullerene Plastic Photovoltaic Devices. *Macromolecules* **2004**, *37*, 2151–2158.
18. Warman, J. M.; de Haas, M. P.; Anthopoulos, T. D.; de Leeuw, D. M. The Negative Effect of High-Temperature Annealing on Charge-Carrier Lifetimes in Microcrystalline PCBM. *Adv. Mater.* **2006**, *18*, 2294–2298.
19. Renu, R.; Ajikumar, P. K.; Advincula, R. C.; Knoll, W.; Valiyaveettil, S. Fabrication and Characterization of Multilayer Films from Amphiphilic Poly(*p*-phenylene)s. *Langmuir* **2006**, *22*, 9002–9008.
20. Renu, R.; Vijila, C.; Ajikumar, P. K.; Hussain, F. S. J.; Ng, K. L.; Wang, H.; Chua, S. J.; Knoll, W.; Valiyaveettil, S. Photophysical Properties of Hydroxylated Amphiphilic Poly(*p*-phenylene)s. *J. Phys. Chem. B* **2006**, *110*, 25958–25963.
21. Nurmawati, M. H.; Renu, R.; Ajikumar, P. K.; Sindhu, S.; Cheong, F. C.; Sow, C H.; Valiyaveettil, S. Amphiphilic Poly(*p*-phenylene)s for Self-Organized Porous Blue-Light-Emitting Thin Films. *Adv. Funct. Mater.* **2006**, *16*, 2340–2345.
22. Renu, R.; Ajikumar, P. K.; Hanafiah, N. B. M.; Knoll, W.; Valiyaveettil, S. Synthesis and Characterization of Luminescent Conjugated Polymer-Silica Composite Spheres. *Chem. Mater.* **2006**, *16*, 1213–1218.
23. Baskar, C.; Lai, Y-H.; Valiyaveettil, S. Synthesis of a Novel Optically Tunable Amphiphilic Poly(*p*-phenylene): Influence of Hydrogen Bonding and Metal Complexation on Optical Properties. *Macromolecules* **2001**, *34*, 6255–6260.
24. Delnoye, D. A. P.; Sijbesma, R. P.; Vekemans, J. A. J. M.; Meijer, E. W. π-Conjugated Oligomers and Polymers with a Self-Assembled Ladder-Like Structure. *J. Am. Chem. Soc.* **1996**, *118*, 8717–8718.

25. Ruoff, R. S.; Tse, D. S.; Malhotra, R.; Lorents, D. C. Solubility of C_{60} in a Variety of Solvents. *J. Phys. Chem.* **1993**, *97*, 3379–3383.
26. Nierengarten, J.-F. Chemical Modification of C_{60} for Materials Science Applications. *New J. Chem.* **2004**, *28*, 1177–1191.
27. Fujita, N.; Yamashita, T.; Asai, M.; Shinkai, S. Formation of C_{60} Fullerene Nanoclusters with Controlled Size and Morphology Through the Aid of Supramolecular Rod-Coil Diblock Copolymers. *Angew. Chem., Int. Ed.* **2005**, *44*, 1257–1261.